Proc. Natl. Acad. Sci. USA
Vol. 93, pp. 1781–1785, March 1996
Biophysics

Observation via one-dimensional $^{13}C^{\alpha}$ NMR of local conformational substates in thermal unfolding equilibria of a synthetic analog of the GCN4 leucine zipper

(coiled coils/protein folding)

EVA G. LOVETT*, D. ANDRÉ D'AVIGNON*, MARILYN EMERSON HOLTZER*, EMORY H. BRASWELL†, DAN ZHU†, AND ALFRED HOLTZER*‡

*Department of Chemistry, Washington University, St. Louis, MO 63130; and †Department of Molecular and Cell Biology and the National Analytical Ultracentrifugation Facility, University of Connecticut, Storrs, CT 06269

Communicated by S. I. Weissman, Washington University, St. Louis, MO, November 2, 1995 (received for review September 21, 1995)

ABSTRACT **Synthesis of a 33-residue, capped leucine zipper analogous to that in GCN4 is reported. Histidine and arginine residues are mutated to lysine to reduce the unfolding temperature. CD and ultracentrifugation studies indicate that the molecule is a two-stranded coiled coil under benign conditions. Versions of the same peptide are made with 99% $^{13}C^{\alpha}$ at selected sites. One-dimensional ^{13}C NMR spectra are assigned by inspection and used to study thermal unfolding equilibria over the entire transition from 8 to 73°C. Spectra at the temperature extremes establish the approximate chemical shifts for folded and unfolded forms at each labeled site. Resonances for each amino acid appear at both locations at intermediate T, indicating that folded and unfolded forms interconvert slowly (>>2 ms) on the NMR time scale. Moreover, near room temperature, the structured form's resonance is double at several, but not all, sites, indicating at least two slowly interconverting, structured, local conformational substates. Analysis of the dynamics is possible. For example, near room temperature at the Val-9, Ala-24, and Gly-31 positions, the equilibrium constant for interconversion of the two structured forms is near unity and the time scale is ≥10–20 ms.**

Protein conformational equilibria are of vital interest in biochemistry and biophysics and are under intense scrutiny in many laboratories. In this endeavor, studies of coiled-coil proteins have attracted increasing attention, both because of the variety of proteins in which the motif occurs and because its structural simplicity recommends it as a model. A two-stranded coiled coil, in which two right-handed α-helices are arranged in parallel and in register and with a slight left-handed super twist, exhibits all the secondary and higher order structural interactions that are so characteristic of proteins but in a simple repetitive geometric context (1). The structure results from a sequential pattern, called a pseudo-repeating heptad (designated *abcdefg*), in which residues *a* and *d* are hydrophobic and *e* and *g* are oppositely charged (1).

A physical understanding of protein conformational equilibria requires elucidation of the population of molecular states. Long coiled coils, such as the tropomyosins from rabbit muscle, show multistate unfolding equilibria whose details are controversial (2, 3). Other tropomyosins (e.g., from chicken gizzard) are thought by some (4) to unfold all-or-none (i.e., to comprise only two kinds of molecular conformations: intact two-stranded coiled coils and random monomer chains), but this too is disputed (5).

For smaller coiled coils, such as the GCN4 leucine zipper (6), calorimetry evidence fits all-or-none unfolding (7). However, an NMR study of ^{1}H–^{2}H exchange at the amide protons shows that individual residues vary in protection over a million fold range (8). Such differences in local dynamics and stability strongly suggest that substates exist. Finally, although the x-ray crystal structure of the GCN4 leucine zipper shows that the two chains are conformationally distinct (9), extant two-dimensional NMR shows only one resonance per proton, indicating that the two chains either become equivalent in solution or rapidly interconvert (10).

Evidence concerning such substates can only come from techniques, such as NMR, that are site-specific and are applied to models small enough to ensure interpretability of the data. To that end, we employ a synthetic, 33-residue capped leucine zipper, GCN4-lzK, which is like that of GCN4 except for four conservative mutations: R1K, H18K, R25K, and R33K. That is, in GCN4-lzK, all basic residues are lysines. This sequence forms a strong coiled-coil dimer and unfolds at a somewhat lower temperature than its parent (see below), making physical studies possible sans denaturants and reducing the danger of thermal damage.

To avoid the complexities of exchange reactions and multidimensional NMR, we synthesized a number of isosequential peptides, differing only in the sites of substitution of 99% $^{13}C^{\alpha}$. This strategy allows examination of conformational species by one-dimensional $^{13}C^{\alpha}$ NMR, using the expected chemical shifts for α-helical and random backbone conformations (11, 12). The high $^{13}C^{\alpha}$ enrichment allows study of dilute solutions, makes peak assignment trivial, and keeps data accumulation times short, thereby assuring reversibility. Moreover, in each peptide, substitution sites can be chosen to minimize spectral overlap. Finally, such isotopic substitutions are conformationally neutral, unlike fluorescent or spin-label probes, which are invariably large hydrophobes.

As will be seen, the one-dimensional $^{13}C^{\alpha}$ NMR spectra of such a series of isotopically substituted, otherwise isosequential peptides reveal that the unfolding equilibrium in this GCN4-leucine zipper analog exhibits not only slowly interconverting local (amino acid level) folded and unfolded conformations but also more than one folded conformation. These one-dimensional spectra therefore contain information not only about the relative populations of these conformations but also about the kinetics of their interconversion.

MATERIALS AND METHODS

For the labeled sites, fluoren-9-ylmethoxycarbonyl (Fmoc) derivatives were prepared (13, 14) from the 99% $^{13}C^{\alpha}$-labeled amino acids (Cambridge Isotope Laboratories, Cambridge, MA), coupled with diisopropylcarbodiimide and 1-hydroxybenzotriazole, and characterized by ^{1}H NMR and HPLC. The isosequential GCN4-lzK peptides were synthesized on a Du-

The publication costs of this article were defrayed in part by page charge payment. This article must therefore be hereby marked "*advertisement*" in accordance with 18 U.S.C. §1734 solely to indicate this fact.

‡To whom reprint requests should be addressed.

Pont RAMPS system using Rapidamide resin (0.1 or 0.05 mmol scale), Fmoc-pentafluorophenyl esters, and acetic anhydride capping. Purification was effected using Vydac (Hesperia, CA) C_{18} columns (10 × 250 and 25 × 250 mm) with a linear gradient of 25–50% acetonitrile containing 0.1% trifluoroacetic acid at 0.3% acetonitrile per min. The products were >95% pure and all had the same retention time on a Vydac analytical C_{18} HPLC column (4.6 × 250 mm). Electrospray mass spectra gave results agreeing with those expected from the sequence within 1 Da.

In this investigation, only glycine and hydrophobic amino acids were labeled, obviating the necessity of blocking side chains. Substitution sites in each peptide were chosen so as to minimize spectral overlap and to provide a broad sampling of chain and heptad locations. Confirmation that all peptides are pure and isosequential was obtained from the ^{13}C NMR spectra. For example, the corresponding chemical shifts are invariant from peptide to peptide and agreed with those in the natural abundance spectrum.

Peptide concentrations were determined from the absorbance due to the lone chain tyrosine, Y17. The extinction coefficient in benign media at 275 nm is 1.40 ± 0.03 (SD, n = 3) $cm^{-1}\cdot M^{-1}$ (M in formality of peptide chains), using the method of Edelhoch (15). The latter is based on the universally observed change in absorbance at 295 nm of unstructured tyrosine (in 6 M guanidinium chloride) when titrated from near-neutral pH to pH 12. The procedure therefore also yields the extinction coefficient of the guanidinium chloride-unfolded GCN4-lzK; we found a value of 1.54 ± 0.01 (SD, n = 3) $cm^{-1}\cdot M^{-1}$ at 275 nm. Most thermal unfolding measurements were performed using the benign, near-neutral saline buffer (100 mM NaCl/50 mM inorganic phosphate, pH 7.4). However, variations in added salt (100–150 mM), buffer concentration (10–100 mM), pH (7.0–7.4), or even the presence of ^2H_2O (to 15%) were shown to have only negligible effects on the thermal unfolding.

CD was measured using a Jasco (Easton, MD) J500A spectropolarimeter controlled by a THE computer via a Jasco IF-500 interface. The instrument was calibrated with (+)-camphor-10-sulfonate by the two-point method (16). Procedures for temperature control and measurement, data acquisition, and analysis have been described (17).

All $^{13}C^{\alpha}$ NMR data were collected at 125.703 MHz, employing a Varian Unity Plus-500 spectrometer with a 10-mm probe and Oxford Instruments temperature controller. Temperatures were independently measured with a thermocouple, using a buffer sample under conditions identical to those in the actual experiments. Approximately 5000 transients were collected at each temperature at a spectral width of 12,686 Hz centered at 44 ppm. The time between transients was 1.3 s (including 0.5-s acquisition time), and excitation pulses of 15 μs (67° flip) were used. Continuous proton decoupling was employed.

For peptide solutions in nondeuterated solvents, the following external lock and reference scheme was used. Prior to data collection on each sample, a dummy ^2H_2O buffer of identical volume (1.8 ml) to the sample was placed in a 10-mm NMR tube and fitted with a 3 mm (o.d.) capillary containing the sodium 3-(trimethylsilyl)-1-propane sulfonate chemical shift reference in ^2H_2O. This sample was shimmed until an acceptable ^1H lineshape was obtained via the decoupler coil. The retained shim settings were used for the actual sample, which was positioned identically in the probe and fitted with a similar capillary as an external field-frequency lock. In this way, ^{13}C half-height linewidths of 6–8 Hz are obtained reproducibly for unfolded peptides (at 73°C) for at least 24 h after shimming.

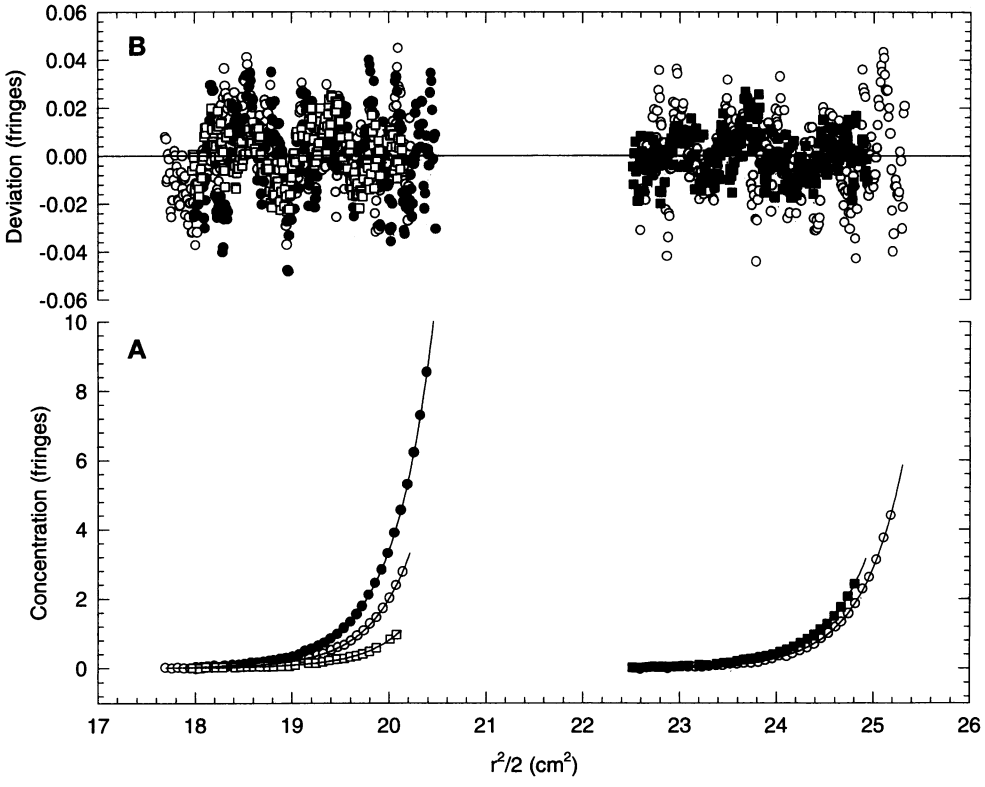

FIG. 1. Equilibrium ultracentrifugation results for GCN4-lzK in near-neutral saline buffer at 4°C. (*A*) Concentration (in fringes; one fringe ≈91 μM chains) vs. one-half the square of the distance (r) from the center of rotation. For clarity, only every fourth data point is shown. Solid lines give theoretical curves for ideal single-species fit (8118 Da) or fit with a predominant (7973 Da) single species and a small amount (1.5%) of higher mass species (best fit). Loading concentrations and rotor speeds are as follows. Low r points (cell top): ●, 330 μM; ○, 82.5 μM at 52,000 rpm; □, 33 μM at 48,000 rpm. High r points (cell bottom): ○, 165 μM at 52,000 rpm; ■, 110 μM at 48,000 rpm. (*B*) Deviation of data from best fit. All points are shown. Symbol types are as in *A*.

Thus, samples can be studied in the absence of extraneous solutes, such as chemical shift reagents or ^2H_2O.

Equilibrium ultracentrifugation employed, as previously described (18), a Beckman model E instrument outfitted with interference optics and a real-time laser-TV system. For low mass species, longer columns than usual (19) are needed to obtain the desired resolution. Hence, special cells were constructed of lucite with two solution–solvent pairs of channels instead of three; these accommodate solution columns up to 5 mm in length and were loaded to 4 mm in our experiments. Equilibrium measurements were made at 4°C on solutions in $NaCl_{150}NaPi_{50}$ (7.4) (aqueous solvents are specified by giving the abbreviation for each solute with millimolarity as a subscript, followed by pH in parentheses) at five concentrations: 330, 165, 110, 82.5, and 33.0 μM in chains and two speeds: 52,000 and 48,000 rpm. The partial specific volume was 0.769 ml/g, as calculated from the amino acid composition (20). The solvent density was found from tables to be 1.0068 g/ml at 4°C.

RESULTS AND DISCUSSION

The ultracentrifugation results are shown in Fig. 1. A global fit (21) to an ideal, monodisperse model yields curves indistinguishable from those drawn on Fig. 1*A* and a molecular mass of 8118 ± 82 Da (SD, 1399 points), which is only 2.9% higher than the expected value (7889 Da) for the two-stranded molecule. However, the residuals (Fig. 1*B*) improve somewhat when fit to a model of such dimers plus a small fraction of material of higher mass. That best fit is the one actually shown in Fig. 1. The resulting molecular mass of the predominant species is 7973 ± 45 Da (SD, 1399 points), which agrees with expectations to 1%. For perspective, we note that, with the polydispersity assumption, the 8118 figure becomes a *z*-average (22), showing that the peptide is over 98% (by weight) two-stranded. These data thus leave no doubt that the relevant molecule under benign conditions is a dimer of GCN4-lzK chains.

CD spectra (not shown) of GCN4-lzK at various temperatures are isodichroic at 203 nm, like other coiled coils (7, 23, 24). CD thermal unfolding curves are shown in Fig. 2 at a variety of concentrations in near-neutral saline buffer. These curves are reversible and therefore describe equilibrium states. As expected for dimeric peptides that dissociate when they unfold, mass action renders the unfolding dependent upon peptide concentration (25). However, the isotopic substitution has no detectable effect; the labeled (filled symbols) and natural abundance (open symbols) samples form one family of curves. Data plotted [e.g., as melting temperature vs. ln(concentration)] all fall on the same curve (data not shown). This underscores the findings from mass spectrometry and NMR (see above) that all these peptides have the same sequence, except for isotopic labeling.

These CD thermal unfolding curves, in which an initial shallow decline is followed by a more precipitous one, are typical of those seen in other coiled coils (6, 25, 26). The shallow decline is thought by some to represent the temperature dependence of CD of an intact coiled coil. It is then used as a baseline for interpretation, often in terms of an all-or-none model, but others ascribe it to progressive unwinding from the ends (26). CD alone cannot distinguish these two possibilities.

Fig. 3 shows one-dimensional $^{13}C^{\alpha}$ NMR spectra for one of our labeled peptides at four of the temperatures determined, covering the full range (8.5–73.0°C); the chain concentration is 300 μM. This peptide bears 99% $^{13}C^{\alpha}$ substitution at four sites: V9 (*a*), L19 (*d*), A24 (*b*), and G31 (*b*), providing the desired broad sampling of chain and heptad (*a–g*) locations.

At 73°C (top spectrum), four sharp resonances appear, which are characteristic of unstructured chains. In contrast, at 8.5°C (bottom spectrum), four prominent resonances, downfield from those at 73°C, establish shifts for folded, coiled-coil

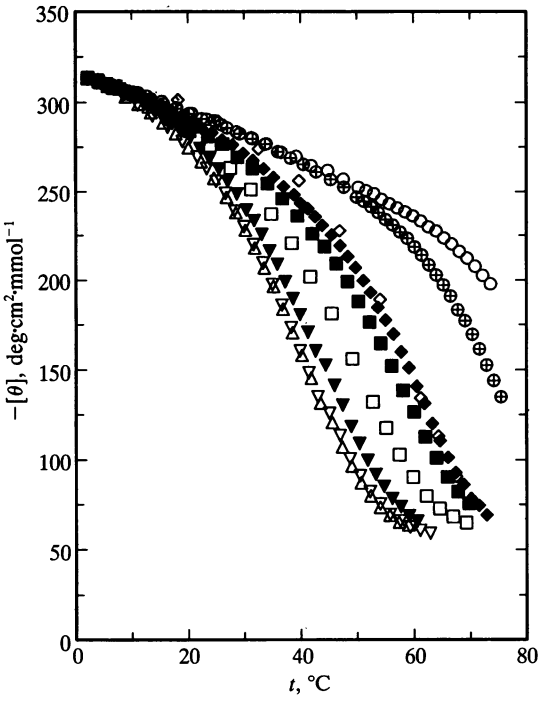

FIG. 2. Mean residue ellipticity at 222 nm vs. temperature for GCN4-lzK at various concentrations in near-neutral saline buffer. Open symbols, natural abundance samples; filled symbols, variously $^{13}C^{\alpha}$ substituted samples. Chain concentrations: ▽, 15.6 μM; △, 16.2 μM; ▼, 25.1 μM; □, 76.1 μM; ■, 142 μM; ◆, 291 μM; ◇, 314 μM; ⊕, 2640 μM; ○, 8520 μM.

species. This low-temperature spectrum provides evidence of interconverting substates, since the G31 (*b*) region also shows a small resonance (≈45.5 ppm) at the location of the corresponding unfolded form. No such resonance appears for the other three sites, although it does (see Fig. 5) for a peptide labeled at L5 (*d*). Thus, there clearly is some unwinding at the coiled coil's ends in this peptide, even at the lowest temperature.

At intermediate temperatures, resonances appear in Fig. 3 at both high- and low-temperature major resonance positions. The way in which these resolved, high- and low-temperature resonances, for a given site, wax and wane reciprocally with increasing temperature indicates that unfolded and folded conformations interconvert slowly on the NMR time scale. This allows determination of site-specific unfolding curves via relative area measurements, after correction for saturation factors. In Fig. 3, only resonances for folded A24 (*b*) and unfolded L19 (*d*) overlap. However, since the other resonance for each stands alone, one can determine the fraction folded at all four sites. Checks are made using labeled peptides with no overlap.

Fig. 3 reveals further conformational complexity. Near room temperature (27.9°C), the folded form's resonance doubles for all but L19 (*d*). Again, these resonances wax and wane reciprocally (15–35°C; data not shown), implying the presence of more than one slowly interconverting *folded* species at those sites. Folded species at V23 (*a*) (data not shown) or L26 (*d*) (see Fig. 5) do not show this duality, nor is it evident in extant proton spectra of the native GCN4 leucine zipper (10). Indeed, to our knowledge, such local interconverting folded substates have not been reported elsewhere for any coiled coil.

Fig. 4 provides further evidence that the resonances at a given chain site represent slowly interconverting conformational forms. These spectra are for the same peptide species of Fig. 3, but all are at 46.9°C. Three concentrations are shown. At this temperature, only one resonance appears at each site

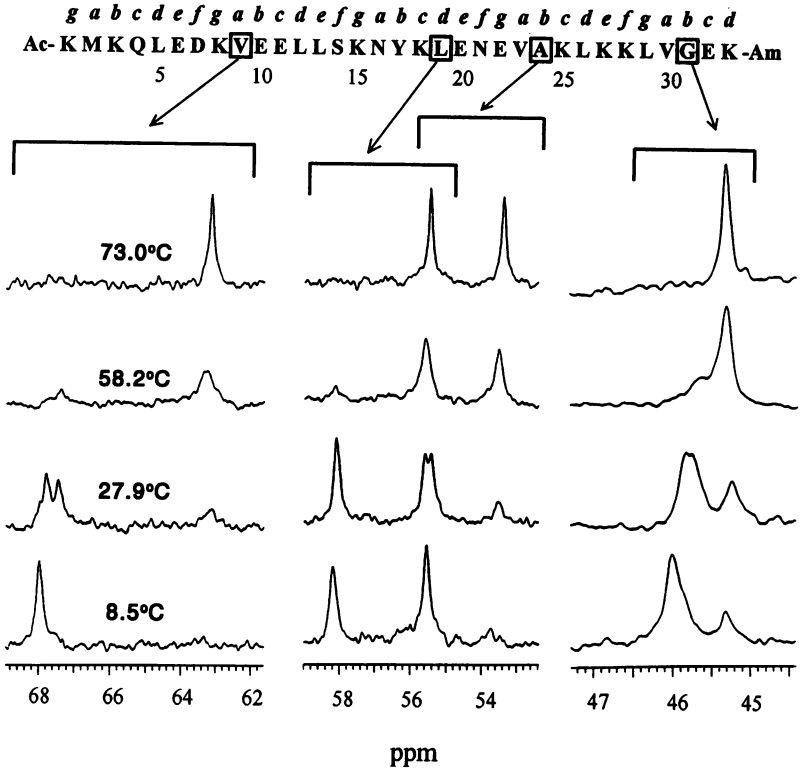

FIG. 3. Proton-decoupled $^{13}C^{\alpha}$ NMR spectra of GCN4-lzK with 99% $^{13}C^{\alpha}$ at V9 (*a*), L19 (*d*), A24 (*b*), and G31 (*b*). Chain formality was 300 μM in near-neutral saline buffer. At the top are the heptad designation, sequence, and residue number. Boxed residues have a $^{13}C^{\alpha}$ substitution. Flat spectral regions have been deleted, and the shift scale has been varied to better reveal resolution.

for the structured form. However, at each site, the resonances of the structured and unstructured forms vary reciprocally with concentration. For V9 (*a*), for example, the peak area for the unstructured form (near 63 ppm) is much less than for the structured form (near 67.5 ppm) at the highest concentration. For the middle concentration, they are more nearly equal. For the lowest concentration, only the resonance for the unstructured form remains. This pattern is repeated at the other sites, again indicating local unfolding that is slow on the NMR time scale.

Fig. 5 shows the leucine $^{13}C^{\alpha}$ NMR region at 27.9°C and 290

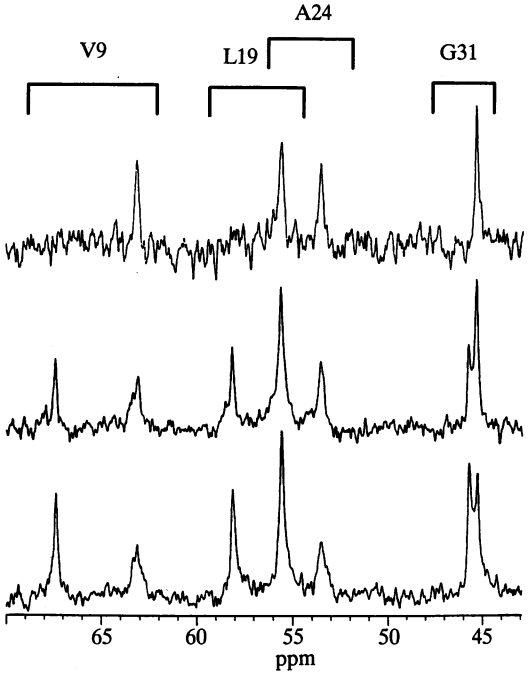

FIG. 4. Proton-decoupled $^{13}C^{\alpha}$ NMR spectra at 46.9°C of GCN4-lzK, isotopically labeled as in Fig. 3. Peptide chain concentrations in near-neutral saline buffer are from top to bottom: 27, 150, and 300 μM. Other conditions are as in Fig. 3.

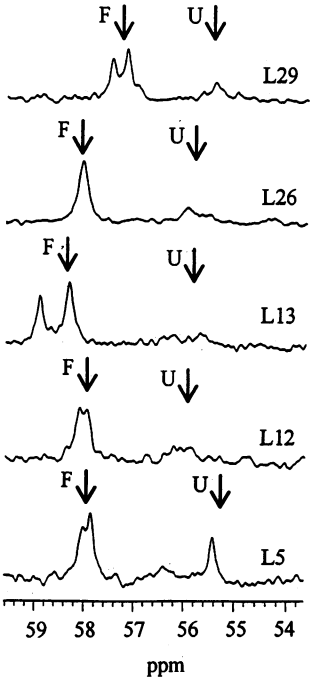

FIG. 5. Leucine region of the $^{13}C^{\alpha}$ NMR spectra at 27.9°C of GCN4-lzK (290 μM in near-neutral saline buffer) variously isotopically labeled. Positions marked F (folded) and U (unfolded) show resonance locations determined from, respectively, low-temperature and high-temperature spectra (data not shown) for the same peptide.

μM for five different isosequential GCN4-lzK peptides, each labeled to avoid overlap. This allows us to compare the behavior of the same residue at different chain locations. Note that the shifts of folded and unfolded forms, as established by low- and high-temperature spectra (data not shown), respectively, are different at different leucine sites. Conformational substates are evidenced by the appearance of site-to-site variations in the fraction unfolded (larger fractions appear at the chain extrema) and by doubling of the folded form's resonance at all but L26 (*d*). Data for the remaining leucine, L19 (*d*), are in Fig. 3 and also show no such doubling.

These spectra contain a great deal of information not only on the local coiled-coil stabilities but also on the time scales of interconversion of one folded species to another and of folded to unfolded species. Even at this early stage, some results are apparent. For example, it is evident, by eye, from Fig. 3 that at V9 (*a*) the areas for the two folded forms are approximately equal near 27.9°C, implying that the equilibrium constant is unity. The forward and reverse rate constants are therefore equal, and a lower bound for the characteristic time can be estimated as follows (27).

The observed separation of the two structured resonances of V9 (*a*) is 0.4 ppm. This corresponds, at 126 MHz, to $\Delta\nu_{obs}$ = 50.4 Hz. However, because of overlap, this is not the true separation of the individual resonances ($\Delta\nu$), which is, in hertz (27),

$$(\Delta\nu)^2 = (\Delta\nu_{obs})^2 + 2(k/\pi)^2, \quad [1]$$

where k is the rate constant. One cannot determine two unknowns with one equation. However, the appearance of the resonance for the V9 (*a*) structured form is very like simulations (27) for which $\Delta\nu = 5k/2\pi$, whereupon we find from Eq. **1** and the observed separation that $\Delta\nu = 61$ Hz and $k \leq 76\ s^{-1}$. The latter corresponds to a time scale of $\geq$13 ms for the interconversion of the two structured forms of V9 (*a*) at 27.9°C. These times are lower bounds because our resonances are inherently broader than in the simulations.

Corresponding estimates can be made for A24 (*b*) and G31 (*b*), but not L19 (*d*); the latter shows only one resonance for the structured form. For A24 (*b*), overlap with the unstructured form of L19 (*d*) is immaterial, since the latter is negligible at 27.9°C. The upshot is that all three doubled sites show equilibrium constants near unity and time scales for interconversion of the two structured forms in the range $\geq$10–20 ms at 27.9°C.

Since the peak separation for the structured and unstructured forms is smallest at G31, it can be used to set a limit on the time scale for their interconversion as well (27). The shift difference at 8.5°C is 0.6 ppm, or 75.5 Hz. Since these are well-separated peaks, $k' << 2\pi\Delta\nu$ must hold (27), implying a time scale far longer than 2 ms. The effect of temperature on the dynamics is seen by comparing the G31 (*b*) regions at 8.5°C (Fig. 3) and 46.9°C (Fig. 4). In the latter, the shift difference for the structured and unstructured forms has been reduced to 0.4 ppm (i.e., 50.4 Hz). Since the highest concentration (300 μM, bottom spectrum of Fig. 4) exhibits approximately equal amounts of each form and mimics simulations (27) for which $\Delta\nu = 5k/2\pi$, we again can estimate the time constant; it is $\geq$13 ms. Thus, the process, as expected, is more rapid at the higher temperature. Extraction of more precise and detailed information is certainly possible but requires further dynamical analysis of our data.

It is perhaps too early to speculate on the precise nature of these substates. The two structured substates found here may be related to the chain inequivalency observed in the dimer by x-ray crystallography (9) and/or to two folded forms postulated in a recent study, by stopped flow, of kinetics of folding a coiled coil having a different sequence (28). The time scale and temperature range found here to connect the two structured forms are similar to those seen in the kinetics study.

Quantitation of these spectra requires methods different from those appropriate in small peptide helices wherein the helix–coil transition is rapid on the NMR time scale (29). However, similarly detailed local unfolding curves should be accessible. Moreover, information on the dynamics of these conformational equilibria is also available in the coiled-coil case, making such studies all the more promising.

This work was supported by Grant GM20064 from the Division of General Medical Sciences, U.S. Public Health Service and a grant from Muscular Dystrophy Association. The ultracentrifugation was supported by National Science Foundation Grant BIR 9318373.

1. Cohen, C. & Parry, D. A. D. (1990) *Proteins* **7,** 1–15.
2. Privalov, P. (1982) *Adv. Protein Chem.* **35,** 1–104.
3. Holtzer, A., Holtzer, M. E. & Skolnick, J. (1990) in *Protein Folding*, eds. Gierasch, L. M. & King, J. (AAAS Books, New York), pp. 177–190.
4. Lehrer, S. S. & Stafford, W. F., III (1991) *Biochemistry* **30,** 5682–5688.
5. Wrabl, J., Holtzer, M. E. & Holtzer, A. (1994) *Biopolymers* **34,** 1659–1667.
6. O'Shea, E. K., Rutkowski, R. & Kim, P. S. (1989) *Science* **243,** 538–542.
7. Thompson, K. S., Vinson, C. R. & Freire, E. (1993) *Biochemistry* **32,** 5491–5496.
8. Goodman, E. M. & Kim, P. S. (1991) *Biochemistry* **30,** 11615–11620.
9. O'Shea, E. K., Klemm, J. D., Kim, P. S. & Alber, T. (1991) *Science* **254,** 539–544.
10. Oas, T. G., McIntosh, L. P., O'Shea, E. K., Dahlquist, F. W. & Kim, P. S. (1990) *Biochemistry* **29,** 2891–2894.
11. Spera, S. & Bax, A. (1991) *J. Am. Chem. Soc.* **113,** 5490–5492.
12. Wishart, D. S., Sykes, B. D. & Richards, F. M. (1991) *J. Mol. Biol.* **222,** 311–333.
13. Schön, I. & Kisfaludy, L. (1986) *Synthesis* **4,** 303–305.
14. Adamson, J. G., Blaskovich, M. A., Groenevelt, H. & Lajoie, G. A. (1991) *J. Org. Chem.* **56,** 3447–3449.
15. Edeloch, H. (1967) *Biochemistry* **6,** 1948–1954.
16. Chen, G. C. & Yang, J.-T. (1977) *Anal. Lett.* **10,** 1195–1207.
17. Holtzer, M. E., Crimmins, D. L. & Holtzer, A. (1994) *Biopolymers* **35,** 125–136.
18. Long, C. G., Braswell, E., Zhu, D., Apigo, J., Baum, J. & Brodsky, B. (1993) *Biochemistry* **32,** 11688–11695.
19. Ansevin, A. T., Roark, D. E. & Yphantis, D. A. (1970) *Anal. Biochem.* **34,** 237–261.
20. Cohen, E. J. & Edsall, J. T., eds. (1943) *Proteins, Amino Acids, and Peptides* (Reinhold, New York), pp. 370–381.
21. Johnson, M. L., Correia, J. J., Halvorson, H. R. & Yphantis, D. A. (1981) *Biophys. J.* **36,** 575–588.
22. Yphantis, D. A. & Lary, J. W. (1994) *SPIE* **2136,** 193–204.
23. Holtzer, M. E. & Holtzer, A. (1992) *Biopolymers* **32,** 1675–1677.
24. Lovett, E. G., d'Avignon, D. A., Holtzer, M. E. & Holtzer, A. (1994) *Protein Sci.* **3,** Suppl. 1, 62.
25. Holtzer, M. E., Holtzer, A. & Skolnick, J. (1983) *Macromolecules* **16,** 173–180.
26. Holtzer, M. E. & Holtzer, A. (1992) *Biopolymers* **32,** 1589–1591.
27. Carrington, A. & McLachlan, A. D. (1967) *Introduction to Magnetic Resonance* (Harper and Row, New York), Chap. 12.
28. Wendt, H., Berger, C., Baici, A., Thomas, R. M. & Bosshard, H. R. (1995) *Biochemistry* **34,** 4097–4107.
29. Shalongo, W., Dugad, L. & Stellwagen, E. (1994) *J. Am. Chem. Soc.* **116,** 8288–8293.